View metadata, citation and similar papers at core.ac.uk
brought to you by CORE
provided by Elsevier - Publisher Connector

Cell PRESS
Immunity
Article

Deficiency of Rap1-Binding Protein RAPL Causes Lymphoproliferative Disorders through Mislocalization of p27kip1

Koko Katagiri,[1,2] Yoshihiro Ueda,[2] Takashi Tomiyama,[3] Kaneki Yasuda,[4] Yoshinobu Toda,[6] Susumu Ikehara,[5] Keiichi I. Nakayama,[7] and Tatsuo Kinashi[2,*]
[1]Department of Life Science, School of Science and Technology, Kwanseigakuen University, and JST, CREST, 2-1 Gakuen, Sanda, Hyogo 669-1337, Japan
[2]Department of Molecular Genetics, Institute of Biomedical Science, and JST, CREST
[3]Division of Gastroenterology and Hepatology, the third Department of Internal Medicine
[4]Department of Urology and Andrology
[5]Department of Stem Cell Disorders
Kansai Medical University, 10-15 Fumizono-cho, Moriguchi, Osaka 570-8506, Japan
[6]Center for Anatomical Studies, Graduate School of Medicine, Kyoto University, Yoshida-Konoe, Sakyo-ku, Kyoto 606-8507, Japan
[7]Department of Molecular and Cellular Biology, Medical Institute of Bioregulation, Kyushu University, 3-1-1 Maidashi, Higashi-ku, Fukuoka 812-8582, Japan
*Correspondence: kinashi@takii.kmu.ac.jp
DOI 10.1016/j.immuni.2010.12.010

SUMMARY

RAPL (an alternative spliced form of *Rassf5*) is a critical Ras-related protein1 (Rap1) effector that regulates lymphocyte adhesion. Here, we have shown that in addition to this previously described function, RAPL also negatively controls lymphocyte proliferation and prevents autoimmunity and lymphoma. RAPL-deficient mice experienced age-related lupus-like glomerulonephritis and developed B cell lymphomas. RAPL-deficient lymphocytes showed hyperproliferation by enhanced S phase entry after antigen receptor ligation. Compared to wild-type cells, RAPL-deficient naive lymphocytes had a 2- to 3-fold increase in Cdk2 kinase activity with a cytoplasmic mislocalization of the cyclin-dependent kinase inhibitor $p27^{kip1}$. RAPL was found to suppress the phosphorylation of $p27^{kip1}$ on serine 10 (S10) and promoted $p27^{kip1}$ nuclear translocation. An S10A mutation in $p27^{kip1}$ corrected its cytoplasmic accumulation, reduced hyperproliferation in RAPL-deficient lymphocytes, and suppressed glomerulonephritis and development of B cell lymphoma. Thus, RAPL serves as a checkpoint for S phase entry to prevent lymphoproliferative disorders through the spatial regulation of $p27^{kip1}$.

INTRODUCTION

The small GTPase Ras-related protein1 (Rap1) regulates multiple functions such as cell proliferation, differentiation, and adhesion (Bos et al., 2001). RAPL was identified as a Rap1-GTP binding protein that mediates Rap1 functions by modulating lymphocyte function-associated antigen-1 (LFA-1) adhesiveness in concert with cell polarization (Katagiri et al., 2003). RAPL is predominantly expressed in immune cells, and RAPL-deficient lymphocytes and dendritic cells have impaired adhesion and motility triggered by chemokines and defective trafficking to peripheral lymph nodes, resulting in hypoplastic lymphoid tissues (Ebisuno et al., 2010; Katagiri et al., 2004). Upon T cell receptor (TCR) ligation, RAPL also mediates important inside-out signal downstream of the Src kinase-associated phosphoprotein 1, SKAP-1 (Raab et al., 2010). In previous studies, we further demonstrated that the Sterile20-like kinase Mst1 is a downstream effector that mediates LFA-1-dependent lymphocyte adhesion upon TCR and chemokine stimulation (Katagiri et al., 2006, 2009).

Rapl (also known as Nore1b) is an alternative spliced form of *Rassf5*, which belongs to a member of the putative tumor-suppressor Rassf family (Avruch et al., 2009). Nore1A, a longer isoform of Rassf5 (Rassf5a) has antiproliferative activity in tumor cell lines (Vos et al., 2003) and epigenetic inactivation of Rassf members including *RASSF5A* (previously also known as *NORE1A*, which has been reported for various types of cancers) (Avruch et al., 2009). Although the Rap1 pathways that affect cell proliferation are thought to be distinct from those that mediate adhesion (Stork and Dillon, 2005), these studies imply that RAPL also controls cell proliferation. However, it is not known whether RAPL regulates cell proliferation in physiological situations or whether RAPL mutations or silencing lead to pathological conditions associated with hyperproliferation and tumor development.

Abnormal cell cycle progression in lymphocytes leads to excessive activation and proliferation and the subsequent loss of self tolerance and development of autoimmunity (Balomenos and Martinez, 2000). Cell cycle progression by cyclins and cyclin-dependent kinases (Cdks) is tightly regulated by Cdk inhibitors (CdkIs) (Sherr and Roberts, 1999). A Cdk2 inhibitor, $p27^{kip1}$ (encoded by the gene *Cdkn1b* and hereafter p27) (Polyak et al., 1994) is a critical regulator of cell cycle progression. p27 forms a complex with Cdk2 and suppresses its kinase activity,

thereby inhibiting the G1 to S phase transition. Antigen receptor stimulation downregulates p27 through ubiquitination and subsequent degradation (Appleman et al., 2000). Defective accumulation of p27 contributes to the induction of T cell anergy and tolerance (Li et al., 2006a). A deficiency in p27 results in enlarged lymphoid organs (Fero et al., 1996; Nakayama et al., 1996). p27 activity is also regulated by subcellular localization p27 (Ekholm and Reed, 2000). p27 shuttles between the nucleus and cytoplasm. To exert its inhibitory function, p27 needs to be transported into the nucleus (Reynisdottir and Massague, 1997). p27 nuclear export is regulated by the exportin CRM1 and ras-related nuclear protein, Ran GTPase, as well as phosphorylation of p27 on serine 10 (Rodier et al., 2001) by protein kinases such as kinase interacting stathmin (KIS) (Boehm et al., 2002), and cytoplasmic translocation of p27 is thought to prevent the assembly of p27 into cyclin E-Cdk2 complexes and to impair the antiproliferative effects of p27 (Boehm et al., 2002; Rodier et al., 2001). Furthermore, genetically targeted mice bearing a p27 mutant unable to interact with cyclin-Cdks exhibit a dominant increase in spontaneous tumorigenesis in many tissues, including lymphomas, compared with *Cdkn1b*$^{-/-}$ mice, indicating an oncogenic function independent of the cyclin-Cdks (Besson et al., 2007). The cytoplasmic localization of p27 in tumor cells, such as B cell lymphomas, has been identified as a mechanism promoting carcinogenesis in humans and mice (Barnouin et al., 1999; Qi et al., 2006). However, the physiological relevance and mechanisms regulating the subcellular localization of p27 in lymphocytes are unclear.

Here, we report that RAPL is important in p27 nuclear localization in both T and B lymphocytes upon antigen receptor stimulation. As a result, RAPL deficiency caused the mislocalization of p27 in the cytoplasm and hyperproliferation of both T and B cells. RAPL-deficient mice developed lupus-like autoimmunity and B cell lymphomas with high frequencies, suggesting that the regulation of p27 subcellular localization by RAPL serves as a checkpoint for S phase entry to prevent immunoproliferative disorders.

RESULTS

Development with Age of Lupus-like Glomerulonephritis and Lymphoma in RAPL-Deficient Mice

We previously reported that young RAPL-deficient mice (<2 months) had hypoplastic spleens and peripheral lymph nodes resulting from reduced lymphocytes. However, approximately 90% of these mutant female mice, but none of control littermates, developed enlarged lymph nodes and spleens at 10 months of age. Total B and T cell numbers were increased by approximately 50%. CD44^{+}CD62L^{-} effector-memory T cells and CD138^{+}B220^{+} plasma cells increased in 10-month-old female RAPL-deficient mice compared to littermate controls (Figure 1A). The aged mutant mice showed a 2-fold increase in serum IgG concentrations relative to wild-type mice and also high titers of antibodies to double-strand DNA (dsDNA) (Figure 1B). Histological examination revealed glomerulonephritis, which was associated with the deposits of IgG and C3 as well as proteinuria (Figures 1B and 1C). Although RAPL-deficient male mice showed similar phenotypes, they were evident at a much later age (15–18 months). There were no significant differences in Foxp3^{+}CD4^{+} regulatory T cell populations between wild-type and RAPL-deficient mice (Figure S1 available online).

In addition, we often found that spleens and lymph nodes in RAPL-deficient mice were extremely large. Histological and flow cytometric analyses indicated that RAPL-deficient mice developed B220^{+}CD19^{+}, diffuse large B cell lymphomas (Figures 1D and 1E). Approximately 30% of RAPL-deficient mice at 1 yr of age but not in control mice developed B cell lymphomas in the peripheral lymph nodes and spleens. Further examination of these lymphomas by flow cytometry indicated that they were an IgM^{+}, IgD^{+}, CD21^{+}, CD23^{+}, and mature B cell type, and that progressed lymphomas often lost these markers to various extents (Figure 1E). They were monoclonal or oligoclonal in origin (Figure 1F). B cell lymphomas in RAPL-deficient mice were not related to the severity of the autoimmune phenotypes.

RAPL-deficient mice also developed tumors in the liver and lung after 1.5 yr of age, although the frequencies of these tumors were lower than the lymphomas (Figure S1B). Histologically, these tumors were identified as hepatocellular carcinomas and lung adenocarcinomas (Figure S1B).

Enhanced S Phase Entry in RAPL-Deficient Lymphocytes

To examine whether RAPL deficiency affects proliferative responses, primary B or T lymphocytes from 7- to 9-week-old wild-type and RAPL-deficient mice were stimulated by antibody crosslinking the antigen receptors. Compared to wild-type B cells, RAPL-deficient B cells displayed enhanced DNA synthesis with various doses of anti-IgM F(ab′)$_2$ (Figure 2A, left). Similarly, RAPL-deficient T cells also showed increased DNA synthesis in response to crosslinking of the TCR complex in the presence or absence of anti-CD28 (Figure 2A, right). Consistent with the hyperproliferative response to anti-IgM F(ab′)$_2$, RAPL-deficient B cells had greater S phase progression compared to wild-type B cells 48 hr after stimulation (41% versus 62%) (Figure 2B). Compared to wild-type T cells, RAPL-deficient T cells also had accelerated S phase entry 48 hr after anti-CD3 stimulation in the presence or absence of anti-CD28 (8% versus 18%, 20% versus 35%) (Figure 2C). There were no changes in apoptotic responses after antigen receptor ligation (data not shown). Thus, RAPL-deficient lymphocytes hyperproliferate in response to antigen receptor ligation.

To demonstrate whether lymphocyte hyperproliferation occurs in vivo, bromo deoxy uridine (BrdU) was injected intraperitoneally into RAPL-deficient mice. As shown in Figure 2D, B cells and CD4^{+} T cells as well as CD8^{+} T cells (data not shown) in lymph nodes of 10-month-old of RAPL-deficient mice bearing no malignancies showed increases in incorporation of BrdU in vivo, compared to those of control lymphocytes, indicating that RAPL deficiency led to lymphocyte hyperproliferation.

Cell Signaling through Antigen Receptors in RAPL-Deficient Lymphocytes

We proceeded to investigate the underlying mechanisms of enhanced lymphocyte proliferation. Because RAPL deficiency does not affect proliferative signaling pathways mediated by mitogen-activated protein (MAP) kinase, nuclear factor-kappa B (NF-κB), or phosphatidyl innositol-3 (PI-3) kinase triggered by the B cell receptor (BCR) or TCR and/or CD28 (Figure S2A),

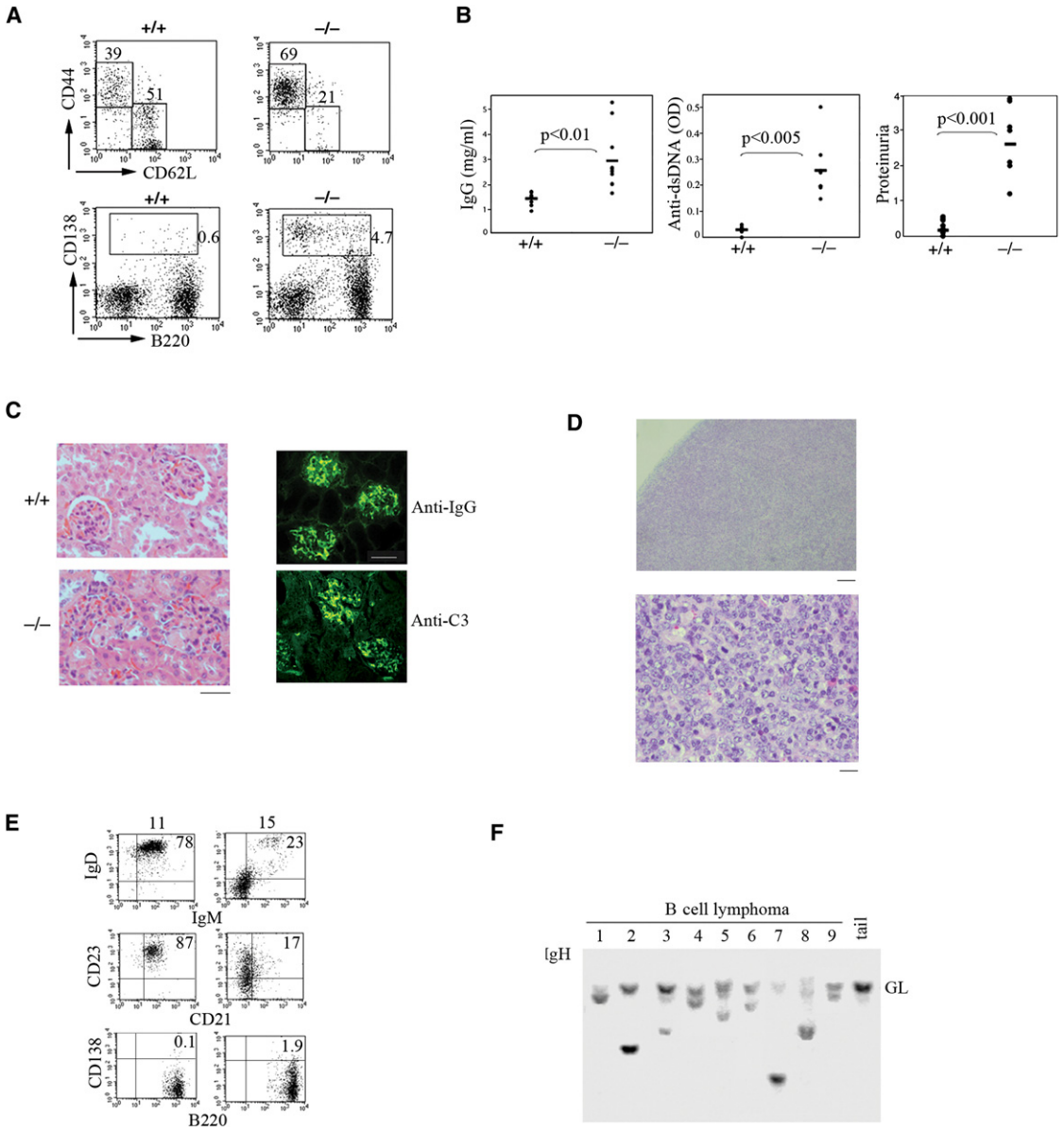

Figure 1. Lupus-like Glomerulonephritis and B Cell Lymphomas in RAPL-Deficient Mice

(A) Flow cytometeric profiles of lymphocytes from spleens of wild-type (+/+) and RAPL-deficient (–/–) mice at 10 months of age. Upper graphs show expression of CD44 and CD62L on $CD4^+$ gated lymphocytes. Lower graphs show expression of CD138 and B220.

(B) Amounts of serum IgG in 12-month-old wild-type (+/+) and RAPL-deficient (–/–) mice. p value for RAPL-deficient mice compared to wild-type control is indicated on the graph (left). Anti-ds DNA titers in 12-month-old wild-type (+/+) and RAPL-deficient (–/–) mice. p value for RAPL-deficient mice compared to wild-type control is indicated on the graph (center). Proteinuria in 12-month-old wild-type (+/+) and RAPL-deficient (–/–) mice. p value for RAPL-deficient mice compared to wild-type control is indicated on the graph (right). Proteinuria was measured with medical color strips dipped in mouse urine and units were defined as follows: 0, no proteinuria; 1, 30 mg/dl; 2, 100 mg/dl; 3, 300 mg/dl; 4, 1000 mg/dl.

(C) Glomerulonephritis with immune complex deposits in RAPL-deficient mice. Hematoxlin-Eosin staining (left) and immunostaining with IgG and C3 complement antibodies (right) of kidney sections from 11-month-old RAPL-deficient mice. Scale bar represents 50 μm.

(D) Low (top) and high (bottom) magnifications of the enlarged lymph nodes from 11-month-old RAPL-deficient mice. Scale bars represent 100 (top) and 10 (bottom) μm, respectively.

(E) Flow cytometric analysis of B cell lymphoma surface phenotypes ($B220^+$, $CD19^+$) developed in RAPL-deficient mice (11 and 15 months old).

(F) Southern blot analysis of *Igh* locus rearrangement in B cell lymphomas. Approximately 30% of RAPL-deficient mice at 1 yr of age developed B cell lymphoma in the peripheral lymph nodes or spleens as shown in Figure 7D. Representative B cell lymphomas independently developed in nine RAPL-deficient mice are shown with tail DNA to indicate the germline (GL) *Igh*.

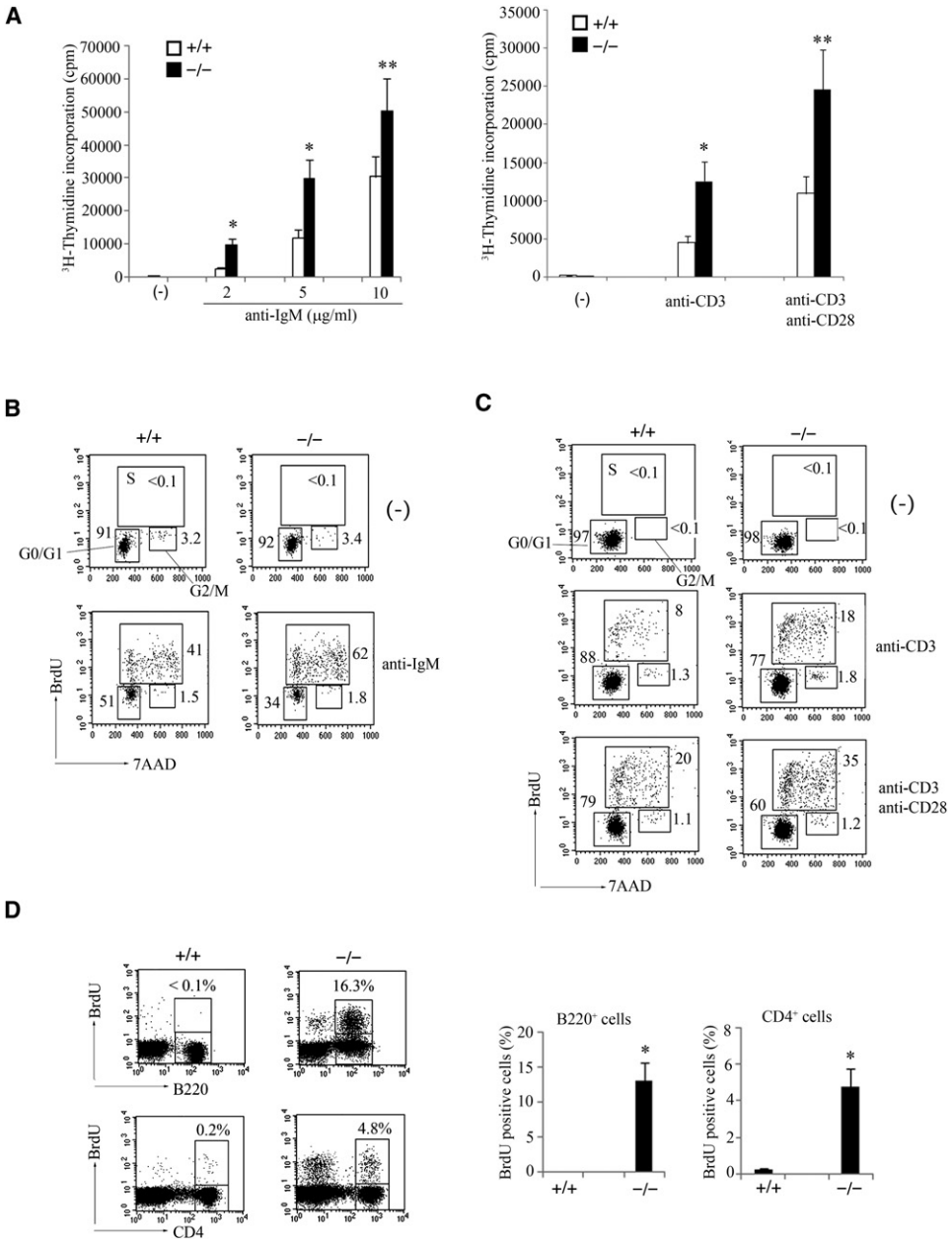

Figure 2. Enhanced Proliferation of RAPL-Deficient Lymphocytes

(A) ^{3}[H]-thymidine uptake by B cells (left) and T cells (right). Primary B and T cells from wild-type (open bar) and RAPL-deficient (closed bar) mice were unstimulated (−) or stimulated with antigen receptor ligation by anti-IgM F(ab′)$_2$ at the indicated concentrations, or by anti-CD3 (5 μg/ml) with or without anti-CD28 (2 μg/ml). ^{3}[H]-thymidine uptake was measured 48 hr after stimulation in triplicate experiments. The mean values and standard errors are shown. *$p < 0.002$, **$p < 0.01$, compared with corresponding wild-type littermate control.

(B and C) Cell cycle profiles of wild-type (+/+) and RAPL-deficient (−/−) B cells (left) or T cells (right) measured at 48 hr without stimulation (−) or with antigen receptor ligation as indicated. The cell populations in each cell cycle phase (G0+G1, S, G2+M) measured by 7AAD and BrdU staining are shown with percentages relative to viable cells in each panel. Data are representative of three independent experiments.

(D) BrdU uptake in vivo. Left: Flow cytometric profiles of BrdU-positive cells in B220$^+$ cells and CD4$^+$ cells of 10-month-old wild-type (+/+) and RAPL-deficient (−/−) mice. Right: Average percentages and standard errors of BrdU incorporated cells for three wild-type (+/+) and RAPL-deficient (−/−) mice are shown. *$p < 0.001$, compared with wild-type littermate control.

we examined cell cycle regulators. Cyclin D and cyclin-dependent kinase 4 (Cdk4) were upregulated and peaked 48 hr after stimulation with anti-BCR or anti-CD3 with or without anti-CD28 (Figure 3A). Cdk4 activity and retinoblastoma (Rb) protein phosphorylation were increased in stimulated B cells and T cells. RAPL-deficient lymphocytes displayed essentially the same amounts of upregulation and activation of cyclin D, Cdk4, and Rb expression and phosphorylation. Similarly, there

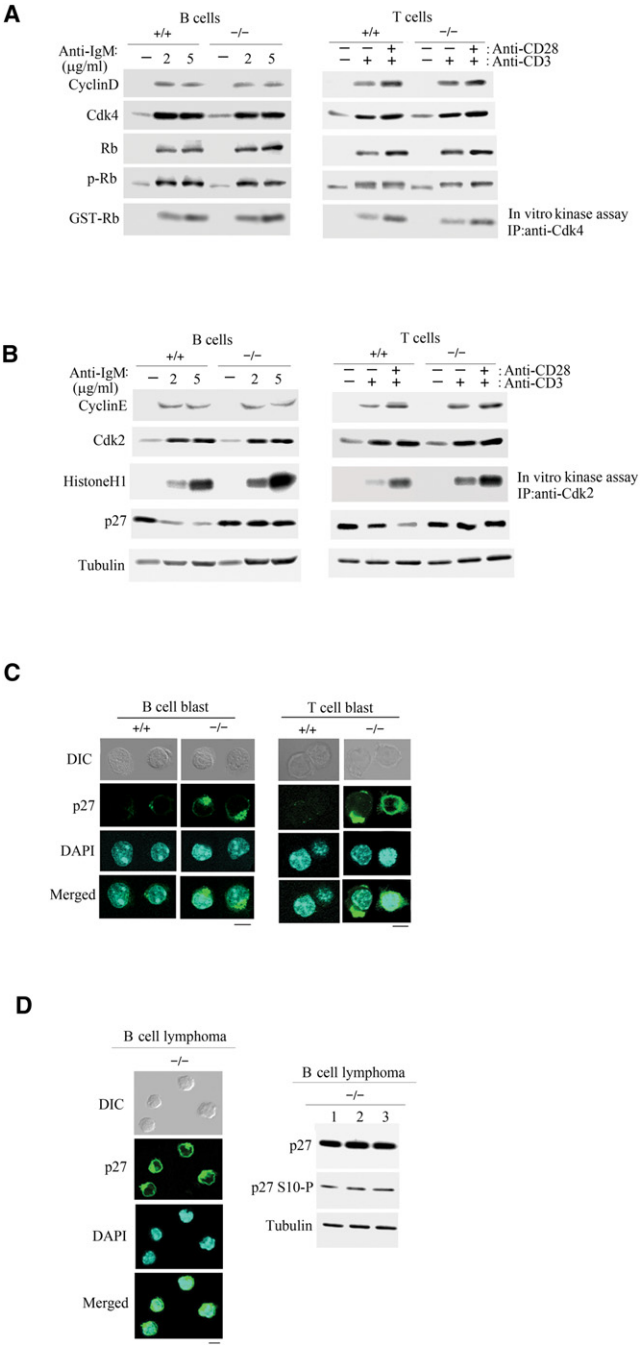

Figure 3. Effects of RAPL Deficiency on Signal Transduction and Cell Cycle Regulators Downstream of Antigen Receptor Signaling

(A) Expression of cyclin D, Cdk4, Rb, and phospho-Rb measured 48 hr after antigen receptor ligation in B (left) and T (right) cells from wild-type (+/+) and RAPL-deficient (−/−) mice. Total lysates derived from 1 × 10^5 cells were applied in each lane. In vitro Cdk4 kinase activities were measured with GST-Rb as a substrate.

(B) Expression of cyclin E, Cdk2, and its kinase activity measured in vitro via phosphorylation of histone H1 as a substrate. Expression of p27 and tubulin in B cells (left) and T cells (right) from wild-type (+/+) and RAPL-deficient (−/−) mice 48 hr after antigen receptor ligation. Total lysates from 1 × 10^5 cells were applied in each lane.

(C) Immunostaining of p27 in wild-type (+/+) and RAPL-deficient (−/−) B and T cell blasts after stimulation with antigen receptor ligation for 2 days. Representative distribution of p27 in lymphocytes is shown. Differential interference contrast (DIC), p27, and DAPI-stained nuclei are indicated. Scale bars represent 5 μm.

(D) Subcellular localization and phosphorylation at serine 10 of p27 in B cell lymphomas. A minimum of 10 independent B cell lymphomas from 10- to 12-month-old RAPL-deficient (−/−) mice were immunostained with anti-p27 or DAPI (nuclei). All B cell lymphomas showed cytoplasmic localization of p27, and a representative example is shown (left). Scale bar represents 10 μm. Immunoblot of total and S10 phosphorylated p27 and tubulin in three independent B cell lymphomas (right).

were no differences in cyclin E and Cdk2 upregulation in both wild-type and RAPL-deficient T and B cells (Figure 3B). However, Cdk2 enzymatic activities in RAPL-deficient B and T cells were augmented at 48 hr compared to wild-type cells after stimulation with anti-BCR (2.6-fold, 2.4-fold) or anti-TCR without (2.5-fold) or with (2.8-fold) anti-CD28 (Figure 3B). These proliferative responses were almost completely inhibited by low doses of a specific Cdk2 inhibitor, CVT-313 (Bhattacharjee et al., 2001), and RAPL-deficient cells tended to be more sensitive to the inhibitor (Figure S2B). These results suggest that Cdk2 drives lymphocyte proliferation and that the enhanced proliferation by RAPL deficiency is largely dependent on Cdk2 activity.

p27, the major Cdk inhibitor for Cdk2, is elevated in G_0 but then downregulated by ubiquitination and proteasomal degradation during the G_0 to S phase transition. In B cells stimulated with anti-BCR, p27 was diminished at 48 hr (Figure 3B). Surprisingly, p27 was not downregulated in RAPL-deficient B cells after 48 hr of stimulation with higher anti-BCR concentrations (5.2-fold compared to wild-type B cells), despite augmented Cdk2 kinase activities (Figure 3B). In wild-type T cells, p27 was downregulated by anti-CD3 and more efficiently by a combination of anti-CD3 and anti-CD28 (Figure 3B), and the degradation was further promoted by the addition of excess amounts of IL-2 (Figure S2C). However, as was the case with RAPL-deficient B cells, there was little to no decrease in p27 by either anti-CD3 or anti-CD3+anti-CD28 (4.1-fold compared to wild-type T cells) at 48 hr, although Cdk2 activities were clearly augmented (Figure 3B). Even excess IL-2 did not promote the degradation of p27 in RAPL-deficient T cells (Figure S2C), although it promoted proliferation of wild-type and RAPL-deficient T cells similarly (data not shown). The amounts of IL-2 in the supernatant of RAPL-deficient T cells were comparable to those in wild-type (Figure S2C), ruling out the possibility that reduced p27 degradation in RAPL-deficient T cells is due to a shortage of IL-2.

Immunostaining of lymphoblasts generated 48 hr after stimulation with antigen receptor ligation revealed that the nuclear p27 was at very low amounts in both WT and RAPL-deficient cells (Figure 3C). Line-profile analysis showed that 4.4% ± 3.5% and 12% ± 8.7% of p27 were present in the nucleus of wild-type B cells and T cells (n = 50), and 5.9% ± 4.7% and 12.6% ± 9.3% in RAPL-deficient B and T lymphoblasts (n = 50) (Figure S3). p27 accumulated predominantly in the cytoplasm of RAPL-deficient T and B cells, although a small amount of p27 remained in the cytoplasm of wild-type cells (Figure 3C; Figure S3). There were no cells with nuclear dominant patterns observed in both wild-type or RAPL-deficient lymphoblasts. Because p27 must be transported into the nucleus to exert its inhibitory action, the cytoplasmic localization of p27 probably

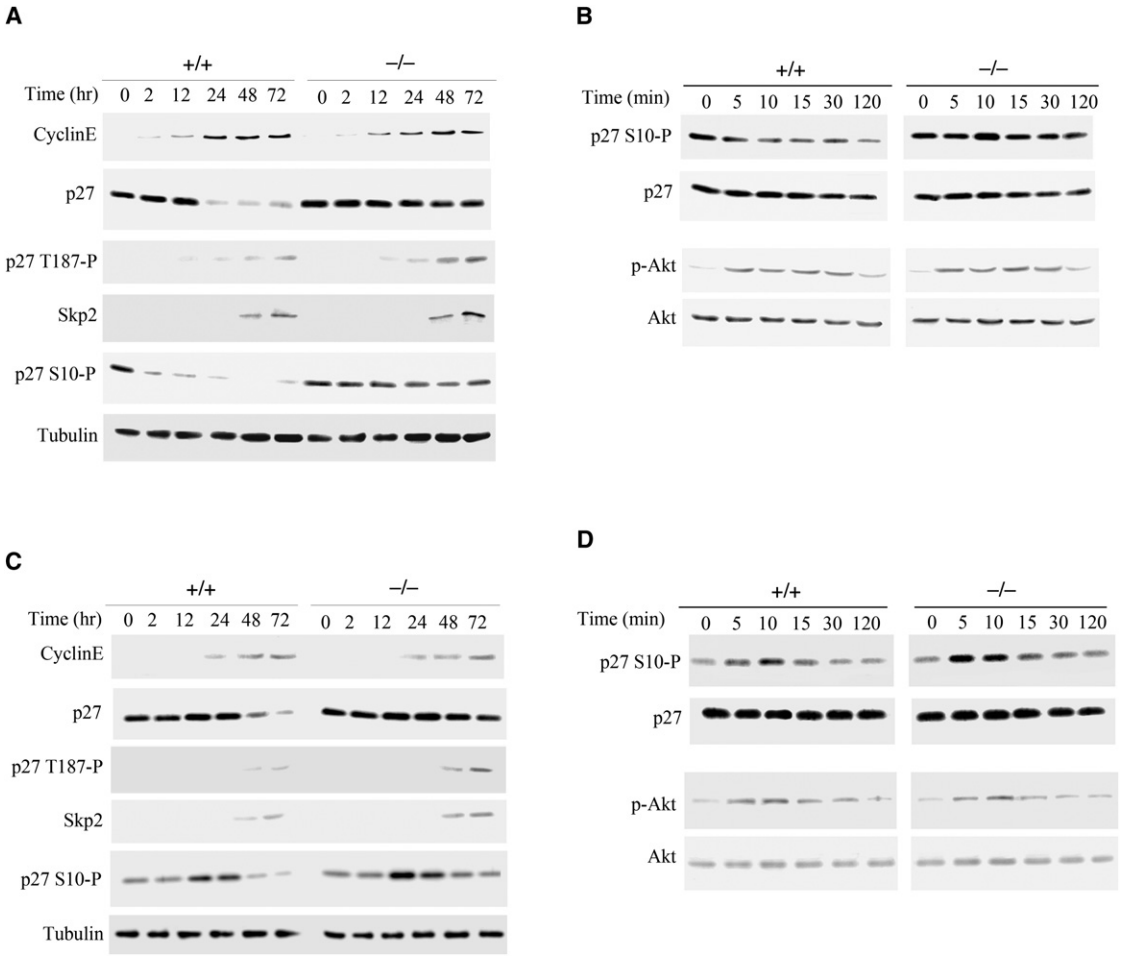

Figure 4. Deregulation of p27 in RAPL-Deficient Lymphocytes

(A) Defective p27 downregulation in RAPL-deficient B cells. Wild-type (+/+) and RAPL-deficient (−/−) B cells were stimulated with anti-IgM $F(ab')_2$ for the indicated times, followed by immunoblot analysis of cyclin E, p27, phosphorylated p27 at threonine 187, Skp2, phosphorylated p27 at serine 10, and tubulin. Total lysates from 1×10^5 cells were applied in each lane.

(B) Kinetics of p27 phosphorylation at serine 10 (S10) in wild-type (+/+) and RAPL-deficient (−/−) B cells after anti-IgM stimulation. Total and S10 phosphorylated p27 and total and phosphorylated Akt are shown. Total lysates from 1×10^5 cells were applied.

(C) Defective p27 downregulation in RAPL-deficient T cells. Wild-type (+/+) and RAPL-deficient (−/−) T cells were stimulated with anti-CD3 and anti-CD28 for the indicated times, followed by immunoblot analysis as in (A).

(D) Kinetics of p27 phosphorylation at serine 10 (S10) in wild-type (+/+) and RAPL-deficient T cells (−/−) after anti-CD3 and anti-CD28 stimulation. Total and S10 phosphorylated p27 and total and phosphorylated Akt are shown. Total lysates from 1×10^5 cells were applied.

renders it inaccessible to a complex of cyclin E and Cdk2, leading to enhanced Cdk2 activities and resistance to degradation.

In all B cell lymphoma generated in RAPL-deficient mice, p27 was abundantly present in the cytoplasm (Figure 3D), as observed in BCR-stimulated RAPL-deficient B blasts (Figure 3C). Line-profile analysis showed that 87.6% ± 3.7% of p27 was present in the cytoplasm. This suggests that the mislocalization of p27 in the cytoplasm underlies lymphoma development.

Kinetics of Phosphorylation and Degradation of p27 in RAPL-Deficient Cells

To investigate whether the mislocalization of p27 in the cytoplasm underlies lymphoproliferative disorders, we examined p27 degradation in more detail. In wild-type B and T cells, p27 declined sharply between 24 and 48 hr after antigen receptor stimulation (Figures 4A and 4C). Cyclin E increased after 12–24 hr and was maintained at high amounts at 24–72 hr. In contrast, RAPL-deficient cells maintained high p27 even at 72 hr poststimulation, whereas cyclin E upregulation was comparable to that in wild-type cells. T187 phosphorylation of p27, a trigger of p27 downregulation, was detected in wild-type cells at 24–72 hr, which coincided with the kinetics of upregulation of cyclin E and Skp2, a substrate-targeting subunit of the SCF ubiquitin ligase complex that regulates entry into S phase (Bashir et al., 2004). RAPL-deficient B and T cells exhibited comparable Skp2 upregulation and essentially the same time course of T187 phosphorylation (Figures 4A and 4C). The ratios of p27 phosphorylated on T187 to total p27 were lower in RAPL-deficient B cells (0.42 at 48 hr) and T cells (0.18 at 48 hr), compared to those of wild-type B cells (0.9 at

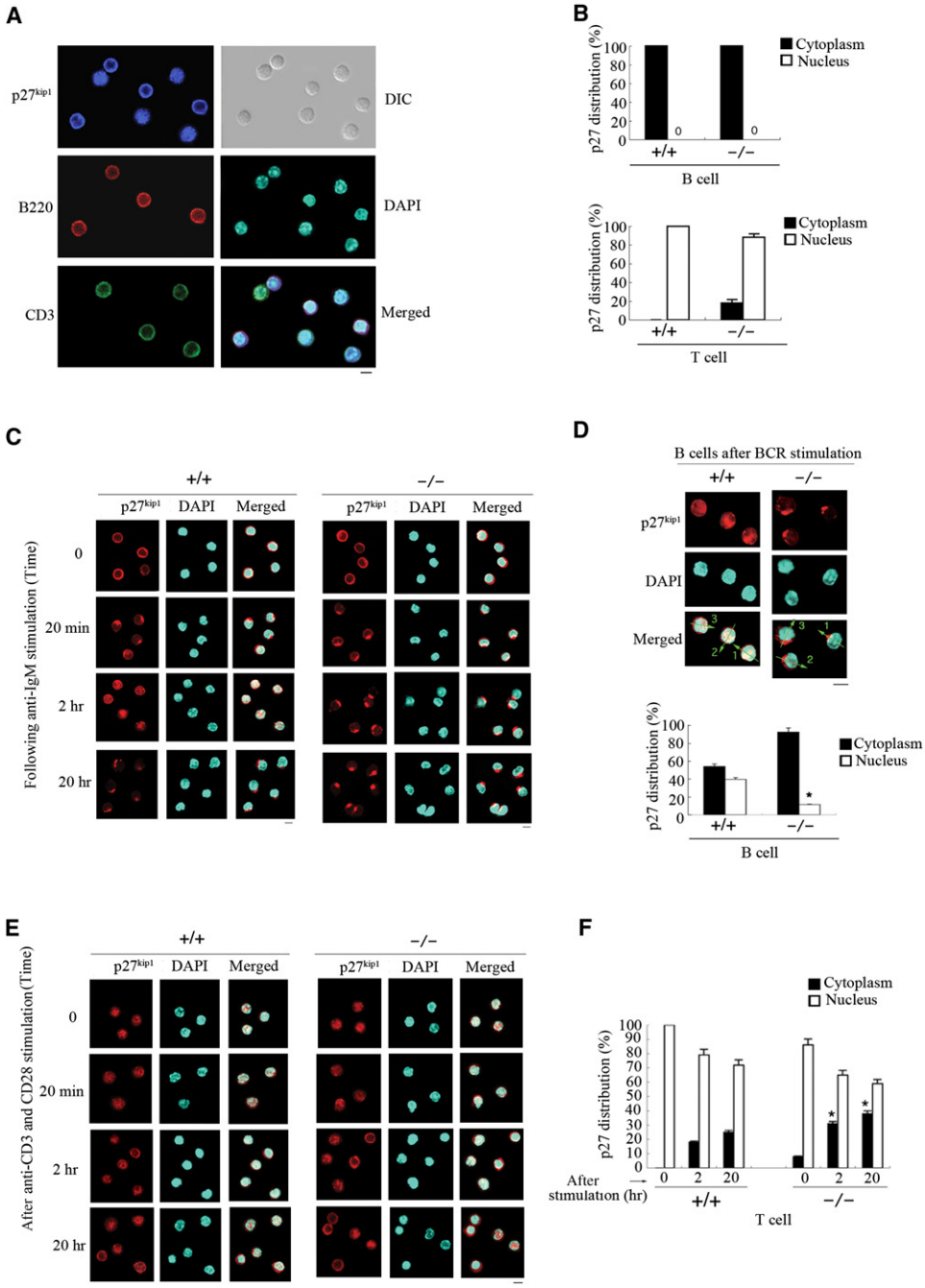

Figure 5. Impaired Redistribution of p27 in RAPL-Deficient B and T Lymphocytes after Antigen Receptor Stimulation

(A and B) Primary lymphocytes from the lymph nodes of wild-type (+/+) and RAPL-deficient (−/−) mice were stained for p27, B220, and CD3. The number of cells with a cytoplasmic and nuclear distribution p27 were visualized and counted by confocal microscopy. At least 100 cells were counted in different microscopic fields. Representative images of p27, B220, CD3, DIC, and DAPI in wild-type cells and average percentages and standard errors for three independent experiments are shown (B). Scale bar represents 5 μm.

(C) Redistribution of p27 in wild-type (+/+) (left) and RAPL-deficient (−/−) (right) B cells. Primary B cells were stimulated with anti-IgM for the indicated times and stained for p27 and nuclei (DAPI). Note that in wild-type B cells, cytoplasmic p27 was translocated into nuclei 2 hr after stimulation before degradation (left), but in RAPL-deficient B cells, cytoplasmic p27 failed to localize in nuclei (right). Scale bars represent 5 μm.

(D) High magnification of cytoplasmic and nuclear distribution of p27 in wild-type (+/+) and RAPL-deficient (−/−) B cells 2 hr after stimulation are shown. Line profiles of p27 and DAPI along the arrows are shown in Figure S5. The average percentages of cells showing nuclear- (open bar) or cytoplasmic- (closed bar) dominant p27 staining in three independent experiments are shown in the lower panel. A minimum of 100 cells were scored per treatment group. *$p < 0.001$, compared with corresponding wild-type littermate control. Scale bar represents 5 μm. The percentages of the nuclear fraction of p27 in the nuclear- and cytoplasmic-dominant population of wild-type B cells were 78.6% ± 6.9% and 36.1% ± 5.5%, and those of RAPL-deficient B cells were 58.5% ± 4.9% and 21.8% ± 2.4%. The difference in the percentages of nuclear p27 between nuclear- and cytoplasmic-dominant population was statistically significant ($p < 0.002$).

48 hr) and T cells (0.22 at 72 hr) (Figures 4A and 4C). The decreased phosphorylation on T187 of p27 might reflect cytoplasmic accumulation of p27 in RAPL-deficient lymphoblasts (Figure 3C; Figure S3), because T187 was mainly phosphorylated by Cdk2-cyclinE in the nucleus (Hara et al., 2001; Lee and Kay, 2007). These data suggest that RAPL deficiency does not affect T187 phosphorylation and Skp2-dependent proteolysis of p27 in the nucleus.

Serine 10 (S10), the major phosphorylation site of p27 (Ishida et al., 2000), is required for cytoplasmic localization at the G_0-G_1 transition in response to mitogenic stimulation (Rodier et al., 2001). S10 phosphorylation was high in resting wild-type B cells, declined to the lowest amounts at 2 and 12 hr poststimulation, and were subsequently undetectable as p27 was degraded (Figure 4A). Resting RAPL-deficient B cells showed similar amounts of S10 phosphorylation; however, S10 phosphorylation did not decrease at 2 and 12 hr poststimulation and were maintained in high amounts levels even at 72 hr (Figure 4A), as well as that of cytoplasmic p27 in B cell lymphoma (Figure 3D). We also examined S10 phosphorylation at early time points after stimulation. In wild-type B cells, S10 phosphorylation was decreased as early as 5 min after stimulation and further declined thereafter (Figure 4B). In contrast, S10 phosphorylation was relatively constant with a slight increase at 10 min in RAPL-deficient B cells (Figure 4B). There were no differences in Akt and Erk phosphorylation in wild-type and RAPL-deficient B cells (Figures 4B; Figure S2A), ruling out the involvement of these kinases in elevated S10 phosphorylation in RAPL-deficient B cells.

T cells showed different magnitudes and patterns of S10 phosphorylation compared to B cells. The S10 phosphorylation in resting T cells were lower than those in resting B cells. S10 phosphorylation was augmented at 12 and 24 hr poststimulation with anti-CD3+anti-CD28 (Figure 4C). RAPL-deficient T cells exhibited similar kinetics of S10 phosphorylation, with approximately 2-fold higher amounts (Figure 4C). When kinetic experiments were performed at early time points, S10 phosphorylation was transiently increased at 5–10 min and returned to basal levels 30 min after anti-CD3 and anti-CD28 stimulation (Figure 4D). RAPL-deficient T cells displayed similar, transient but enhanced S10 phosphorylation (Figure 4D). Stimulation with anti-CD3 alone induced S10 phosphorylation almost comparable to that by anti-CD3 and anti-CD28 (Figure S4A), indicating that phosphorylation of p27 at S10 is mainly regulated through TCR signaling. Thus, enhanced phosphorylation on S10 occurs at 5–10 min and 12–24 hr after stimulation in RAPL-deficient T cells, which precedes degradation of p27 and the entry to S phase. Again, there were no changes in Akt and Erk phosphorylation in RAPL-deficient T cells (Figure 4D; Figure S2A). Collectively, these results suggest that RAPL deficiency specifically upregulates S10 phosphorylation that is important for the cytoplasmic localization of p27 in lymphocytes.

Because IL-7 has been reported to stimulate proliferation through enhanced p27 destabilization in an IL-7-dependent thymocyte cell line (Li et al., 2006b), we examined the effect of IL-7 on S10 phosphorylation. IL-7 augmented proliferation of T cells from wild-type and RAPL-deficient mice to the same extent (approximately 4-fold) in the presence of anti-CD3 (Figure S4B). IL-7 did not affect S10 phosphorylation in both wild-type and RAPL-deficient T cells (Figure S4C), indicating that IL-7 enhanced proliferation independently of RAPL.

Mislocalization of p27 in the Cytoplasm of RAPL-Deficient Cells

We next examined p27 redistribution in primary lymphocytes by immunostaining. Unexpectedly, resting T and B lymphocytes exhibited distinct p27 distribution patterns: in B cells p27 was predominantly cytoplasmic (83.5% ± 3% of p27), but in T cells, the majority of p27 was localized in the nucleus (94.2% ± 1.2% of p27) (Figure 5A). Quantitative results showed that the distribution of p27 in the cytoplasm was essentially the same in resting wild-type and RAPL-deficient B cells (Figure 5B). Similar to wild-type T cells, most RAPL-deficient T cells also showed nuclear localization of p27 with a minor population showing cytoplasmic localization (Figure 5B).

After anti-BCR stimulation, p27 was dynamically redistributed in wild-type B cells. p27 rapidly clustered in the cytoplasm near the nucleus 20 min after stimulation and relocated into the nucleus at 2 hr (Figure 5C). Quantitative analysis showed that p27 distribution was predominantly nuclear in approximately 40% of the population at 2 hr (Figure 5D; Figure S5A). At 20 hr, the amount of p27 in the nucleus decreased with some remaining in the cytoplasm (Figure 5C; Figure S5B). In RAPL-deficient B cells, p27 also rapidly clustered in the cytoplasm (Figure 5C). However, in more than 80% of cells, p27 failed to localize to the nucleus at 2 hr and remained abundant in the cytoplasm at 20 hr (Figures 5C and 5D; Figure S5). Preferential decrease of p27 in the nucleus with residual p27 in the cytoplasm of wild-type B cells suggested that p27 degradation occurs mostly in the nucleus and that RAPL deficiency impaired a step in p27 nuclear translocation in B cells. The subcellular location of p27 is consistent with S10 phosphorylation kinetics and amounts.

Although a majority of p27 was present in the nucleus of resting wild-type T cells, a fraction of p27 was also cytoplasmic in most T cells 20 min after anti-CD3 and anti-CD28 stimulation, and 20% of the T cells exhibited the cytoplasmic-dominant distribution of p27 at 2 hr (Figures 5E and 5F). Meanwhile, the cytoplasmic-dominant population was almost doubled

(E) Redistribution of p27 in wild-type (+/+) (left) and RAPL-deficient (right) T cells. Primary T cells were stimulated with anti-CD3 and anti-CD28 for the indicated times and stained for p27 and nuclei (DAPI), as in (C). Note that a portion of nuclear p27 was translocated into the cytoplasm after stimulation in both wild-type and RAPL-deficient T cells, but cells showing predominantly cytoplasmic p27 increased in RAPL-deficient T cells compared with wild-type T cells. Scale bar represents 5 μm.

(F) The average percentages of cells showing nuclear- (open bar) or cytoplasmic- (closed bar) dominant p27 in three independent experiments are shown. Wild-type (+/+) and RAPL-deficient T cells were stimulated for 2 hr or 20 hr with anti-CD3+anti-CD28. A minimum of 100 cells were scored per treatment group. *$p < 0.005$, compared with corresponding wild-type littermate control. The percentages of cytoplasmic p27 in the cytoplasmic and nuclear-dominant population of wild-type T cells were 62.5% ± 5.6% and 17.9% ± 11.3%, and those of RAPL-deficient T cells were 66.1% ± 6.0% and 25.6% ± 15.2%. The difference in the percentages of cytoplasmic p27 between cytoplasmic- and nuclear-dominant population was statistically significant ($p < 0.001$).

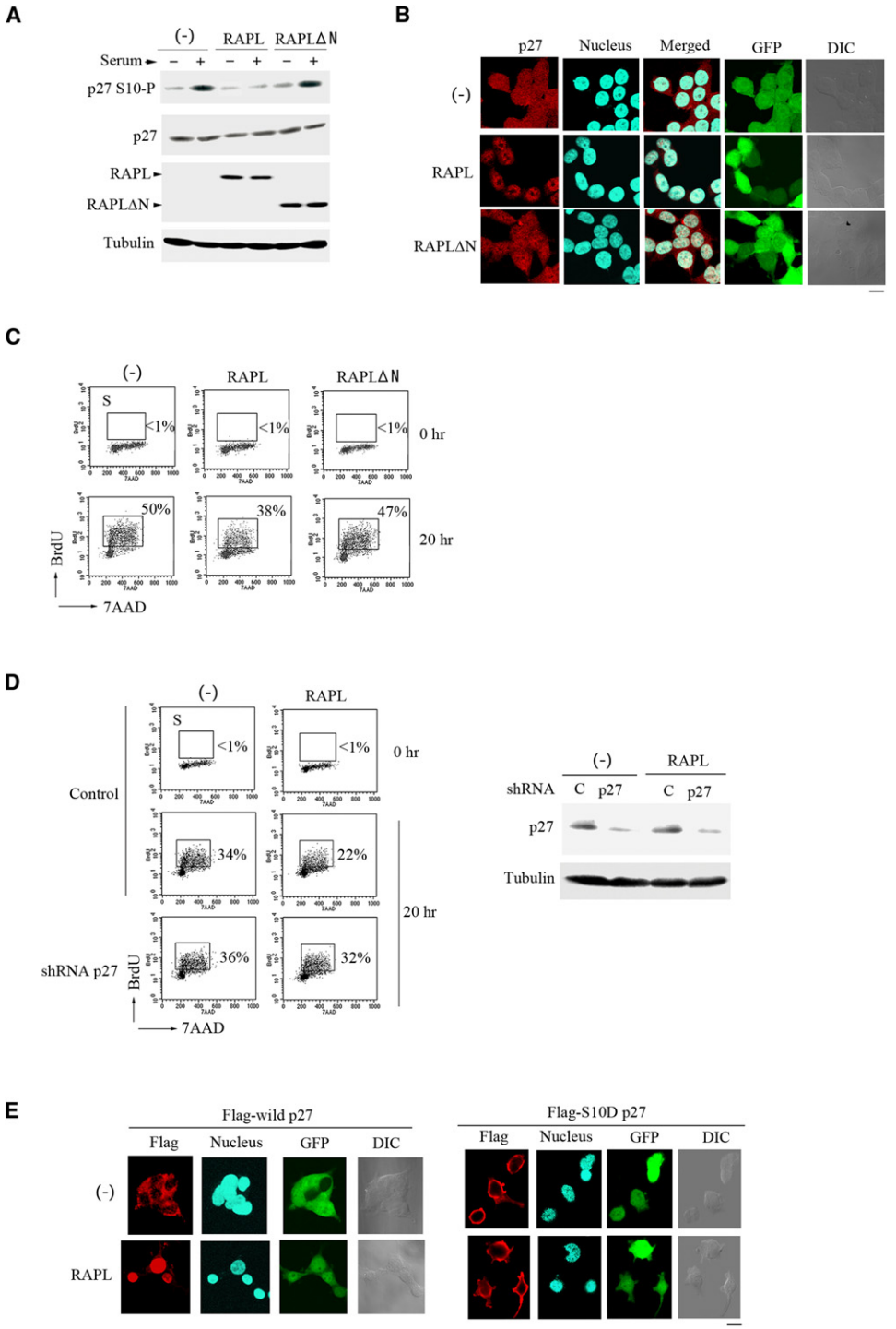

Figure 6. RAPL Promotes p27 Nuclear Localization and Suppresses S Phase Entry

(A) RAPL mutant did not inhibit p27 phosphorylation on S10. 293T cells with or without RAPL or RAPLΔN expression were serum starved for 2 days and then stimulated with 10% serum for 5 hr. Total and S10 phosphorylated p27, myc-RAPL or myc-RAPLΔN, and tubulin are shown. Total lysates derived from 1×10^4 cells were applied in each lane.

(B) Inhibition of p27 nuclear export by RAPL but not RAPLΔN. 293T cells were transfected with GFP alone (–), RAPL, or RAPLΔN plus GFP (green) and then stimulated with serum for 5 hr after serum starvation for 2 days. Cells were immunostained for p27 (red) and DAPI (nuclei). Scale bar represents 10 μm.

(C) Cell cycle analysis of 293T cells without (–) or with RAPL or RAPLΔN expression before or after serum stimulation for 20 hr. The percentage of cells labeled with BrdU (S phase) is shown in each panel. The results are representative of three independent experiments.

(D) Cell cycle analysis of control or p27-specific shRNA transfected 293T cells without (–) or with RAPL expression before or after serum stimulation for 20 hr. The percentage of cells labeled with BrdU (S phase) is shown in each panel. The results are representative of three independent experiments

in RAPL-deficient T cells 2 hr and 20 hr after stimulation (Figures 5E and 5F). The similar increase in the cytoplasmic-dominant distribution was observed in RAPL-deficient T cells at 2 hr after stimulation with anti-CD3 alone (data not shown). Thus, these results indicate the possibility that RAPL modulates the cytoplasmic localization of p27 through S10 phosphorylation.

Inhibition of p27 S10 Phosphorylation and Enhanced Nuclear Localization by RAPL

To examine whether RAPL modulates S10 phosphorylation and subcellular localization of p27, we employed a heterologous system by using 293T cells, which are well characterized for nuclear export of p27 (Boehm et al., 2002; Ishida et al., 2002). S10 was basally phosphorylated in serum-starved 293T cells, increased at 0.5 hr after serum stimulation, and then peaked at 1–5 hr to amounts similar to that in continuously growing cells (Figure S6A). In contrast, in serum-starved RAPL-transfected 293T cells, basal and serum-induced S10 phosphorylation was severely diminished (Figure S6A). In loss-of-function mutant lacking the N-terminal half (RAPLΔN) (Katagiri et al., 2003)-transfected 293T cells, serum-induced S10 phosphorylation was not decreased (Figure 6A). At 5 hr after serum addition, 51.2% ± 3.1% of p27 was cytoplasmic in control cells. Under the same conditions, 82.2% ± 7.4% of p27 was nuclear in RAPL-expressing cells with very low amounts in the cytoplasm, but this effect was not observed in RAPLΔN-expressing cells (Figure 6B), consistent with the S10 phosphorylation amounts of p27 (Figure 6A). RAPL, but not RAPLΔN expression, reduced the frequency of cells in S phase at 20 hr after serum stimulation (Figure 6C). This reduction was abrogated by p27 silencing (Figure 6D), indicating that the inhibitory effect of RAPL on proliferation depends on p27.

We also confirmed the similar effects of RAPL on p27 localization by using CH27 B cell lymphoma cells. RAPL expression promoted nuclear localization and significantly decreased cell proliferation (Figure S6B). This suppressive effect of RAPL on proliferation was also abrogated by p27 silencing (Figure S6B).

If RAPL could promote nuclear localization of p27 through suppression of S10 phosphorylation, cytoplasmic localization of a phosphomimetic mutant p27S10D (Ishida et al., 2000) should not be affected by RAPL. To examine this possibility, Flag-tagged p27 and p27S10D were transfected into control and RAPL-expressing cells. The cells were synchronized by serum starvation, then added to serum for 6 hr before staining. Wild-type p27 was localized in the cytoplasm of control cells, whereas it was mainly present in the nucleus of RAPL-expressing cells, as is the case with endogenous p27 (Figure 6E). In contrast, approximately 90% of p27S10D was localized in the cytoplasm of both control and RAPL-expressing cells (Figure 6E), indicating that S10D is dominant over RAPL for p27 localization. This provides further support for the notion that RAPL regulates p27 localization through suppression of S10 phosphorylation.

Because kinase interacting stathmin (KIS) was reported to phosphorylate S10 in the G1 phase (Boehm et al., 2002), we investigated whether RAPL could inhibit KIS kinase activity. The Flag-tagged mouse KIS and RAPL were cotransfected into 293 T cells, and we examined immune-complex kinase activity of KIS by using p27 and p27S10A protein as a substrate. KIS phosphorylated the wild-type p27 but not the p27 mutant in which serine 10 is substituted with alanine (p27S10A) (Figure S6C), as reported (Boehm et al., 2002). RAPL expression reduced the kinase activity of KIS on S10 by 60% (Figure S6C). Meanwhile, silencing of KIS in 293T cells increased nuclear-dominant localization of p27, as previously reported (Boehm et al., 2002), and RAPL overexpression had marginal effects on the nuclear localization of p27 in KIS-silenced 293T cells (data not sown). This result suggests that RAPL could decrease the phosphorylation of p27 on S10 at least through the suppression of KIS activity.

The S10A Mutation in $p27^{kip1}$ Suppresses Autoimmunity and B Cell Lymphoma in RAPL-Deficient Mice

If the growth stimulatory effect of RAPL deficiency is mediated by S10 phosphorylation of p27, it would be expected that the S10A mutation could counteract its effect and prevent lymphoproliferative diseases of RAPL-deficient mice. To examine this possibility, we crossed p27S10A genetically targeted mice (Kotake et al., 2005) with RAPL-deficient mice to generate *Cdkn1b*$^{S10A/S10A}$ RAPL-deficient mice (Figure 7A). As shown in Figure 7B, the S10A mutation in p27 significantly reduced the $CD138^{+}B220^{+}$ plasma cells by 67% and $CD44^{+}CD62L^{-}$ effector-memory T cells by 28%. Accordingly, the titers of antibodies to double-stranded DNA (dsDNA) decreased by 58%, the incidence of proteinuria was reduced (63% versus 22%), and also deposition of IgG was rarely detected (Figure 7C; Figure S7A), indicating that the S10A mutation suppressed the development of severe glomerulonephritis in 10-month-old RAPL-deficient mice. Importantly, B cell lymphoma and other tumors did not develop in *Cdkn1b*$^{S10A/S10A}$ RAPL-deficient mice (Figure 7D; Figure S7B).

In resting *Cdkn1b*$^{S10A/S10A}$ B cells sufficient or deficient for RAPL, p27 was mainly located in the cytoplasm as seen in the wild-type situation, although its distribution tended to be aggregated near the nucleus (Figure 7E). In *Cdkn1b*$^{+/+}$ RAPL-deficient B cells, p27 remained in the cytoplasm after stimulation (Figure 5C). In contrast, when *Cdkn1b*$^{S10A/S10A}$ RAPL-deficient B cells were stimulated with anti-IgM, p27S10A translocated into the nucleus in both RAPL-sufficient and -deficient B cells with comparable numbers of cells showing nuclear-dominant p27 (Figure 7E; Figure S7C). p27 degradation in *Cdkn1b*$^{S10A/S10A}$ RAPL-deficient B cells was greatly accelerated compared to that of *Cdkn1b*$^{+/+}$ RAPL-deficient B cells (Figure S7D), and the level of degradation was almost equivalent to that of wild-type B cells (Figure 3B). *Cdkn1b*$^{S10A/S10A}$ RAPL-deficient B cells did not exhibit enhanced proliferation with anti-IgM, compared to

(left). Immunoblot of p27 and tubulin in RAPL or vector control (−) expressing 293T cell lysates after control-(c) or p27-specific (p27) shRNA transfection (right).

(E) A S10D mutation of p27 inhibited the nuclear localization of p27 by RAPL. 293T cells were transfected with flag-tagged wild-type or S10D mutant p27 together with GFP alone (−) or RAPL plus GFP (green), and then stimulated with serum for 5 hr after serum starvation for 2 days. Cells were immunostained for flag (red) and DAPI (nuclei). Scale bar represents 10 μm.

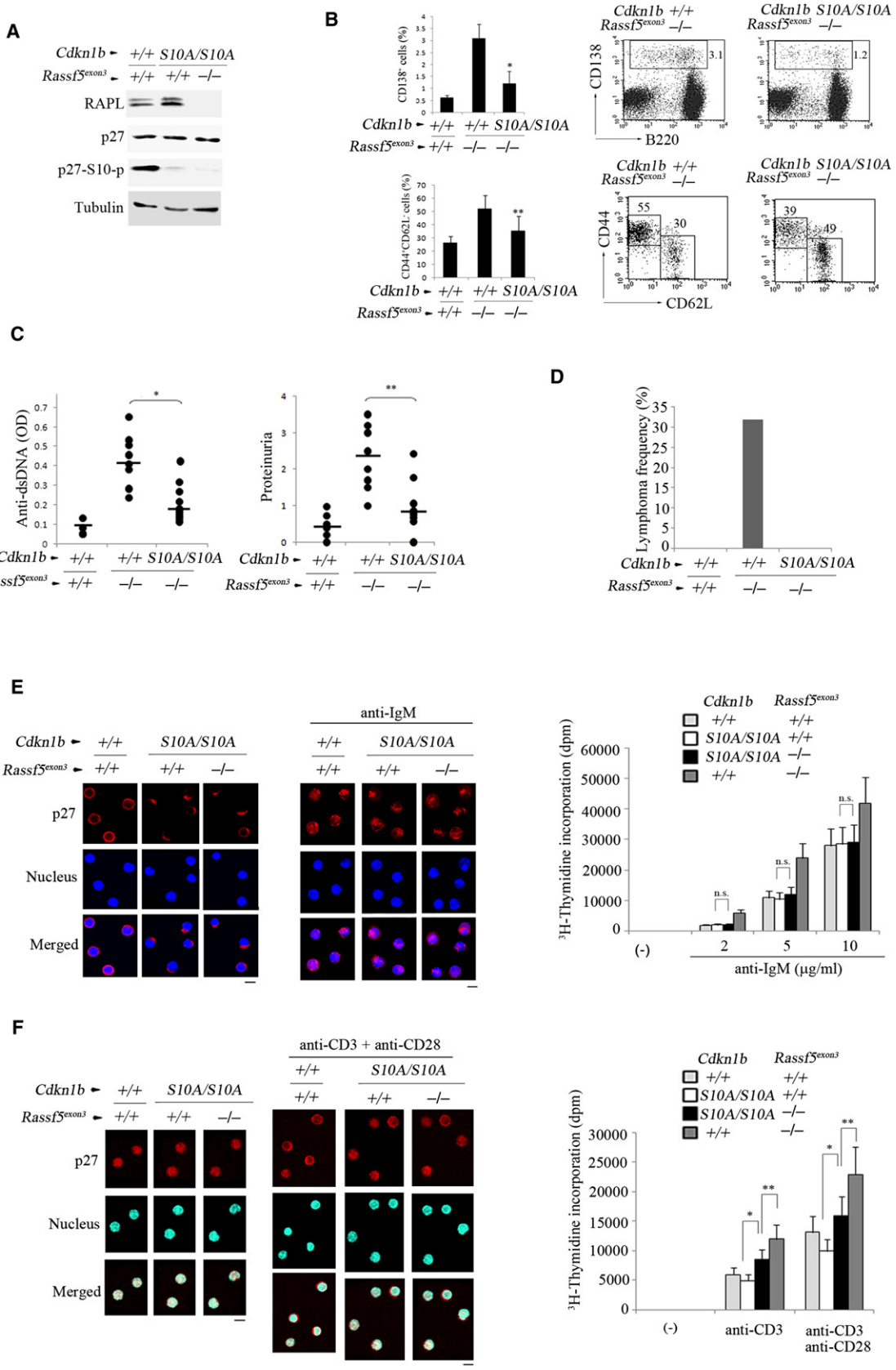
A
Cdkn1b +/+ S10A/S10A
Rassf5exon3 +/+ +/+ −/−
RAPL
p27
p27-S10-p
Tubulin
B
CD138+ cells (%)
Cdkn1b +/+ +/+ S10A/S10A
Rassf5exon3 +/+ −/− −/−
CD44+CD62L cells (%)
Cdkn1b +/+ Rassf5exon3 −/−
Cdkn1b S10A/S10A Rassf5exon3 −/−
CD138
B220
3.1
1.2
CD44
CD62L
55
30
39
49
C
Anti-dsDNA (OD)
Proteinuria
D
Lymphoma frequency (%)
E
anti-IgM
p27
Nucleus
Merged
3H-Thymidine incorporation (dpm)
anti-IgM (μg/ml)
n.s.
F
anti-CD3 + anti-CD28
anti-CD3
anti-CD3 anti-CD28

those of *Cdkn1b*$^{S10A/S10A}$ RAPL-sufficient B cells and wild-type B cells (Figure 7E). Thus, S10A mutation corrected B cell abnormalities.

In *Cdkn1b*$^{S10A/S10A}$ T cells sufficient or deficient for RAPL, p27 was mainly located in the nucleus, as is the case with *Cdkn1b*$^{+/+}$ T cells (Figure 7F). When stimulated with anti-CD3 and anti-CD28, the proportion of the cells expressing p27S10A translocated into the cytoplasm was lower than that of the cells with wild-type p27 (21.4% versus 33.1%) (Figure 7F; Figure S7C). There was no significant increase of RAPL-deficient T cells with cytoplasmic-dominant localization of p27S10A (20.6%) (Figure 7F; Figure S7C). p27 degradation in *Cdkn1b*$^{S10A/S10A}$ RAPL-deficient T cells was also enhanced compared to that of *Cdkn1b*$^{+/+}$ RAPL-deficient T cells (Figure S7D), and the amount of downregulation was almost equal to that of wild-type T cells (Figure 3B). The cytoplasmic mislocalization of p27 in *Cdkn1b*$^{+/+}$ RAPL-deficient T cells with anti-CD3 was also corrected with S10A mutation on p27 (Figure S7E). These results indicate that the mislocalization and degradation of p27 in RAPL-deficient T cells was dependent on S10 phosphorylation. T cells from *Cdkn1b*$^{S10A/S10A}$ RAPL-deficient T cells exhibited lower proliferation compared to *Cdkn1b*$^{+/+}$ RAPL-deficient T cells, but it was still significantly higher than *Cdkn1b*$^{S10A/S10A}$ RAPL-sufficient T cells (Figure 7F). These data suggest that hyperproliferation of T cells by RAPL deficiency was partly dependent on S10 phosphorylation, although other mechanisms are probably involved.

All together, these results demonstrate that RAPL-dependent regulation of phosphorylation of p27 on S10 plays important roles for prevention of lupus-like glomerulonephritis and B cell lymphoma.

DISCUSSION

Our results demonstrated a role for RAPL in suppression of S10 phosphorylation of p27 and nuclear export of p27, thereby retarding the G1-S phase transition. The defective checkpoint in the G1-S transition resulting from RAPL deficiency enhanced proliferation, leading to lupus-type glomerulonephritis and lymphomas. p27S10A genetic targeting in the RAPL-deficient background rescued both glomerulonephritis and B cell lymphoma and demonstrates that S10 phosphorylation of p27 is critical for the development of lymphoproliferative diseases by RAPL deficiency.

Our results suggest that mislocalized p27 leads to increased Cdk2 activity, which in turn promotes G1-S phase transition in lymphocytes. It was reported that Cdc2 plays a role in S-phase entry in the absence of Cdk2 (Aleem et al., 2005). p27 also associates with and inhibits Cdc2 (Aleem et al., 2005). The experiment with a Cdk2 inhibitor favors the major role of Cdk2 in S phase entry of normal lymphocytes, although prolonged Cdk2 deficiency might lead to compensation with Cdc2. In either case, it is possible that RAPL suppresses both Cdk2 and Cdc2 activity through the promotion of p27 nuclear localization and regulates S phase entry of lymphocytes after stimulation through antigen receptors.

The S10 mutation of p27 completely abrogated the hyperproliferative responses of RAPL-deficient B cells, but partially inhibited those of RAPL-deficient T cells, indicating that other mechanisms operate in RAPL-deficient T cells. Mst1 is activated by Rap1 and RAPL and responsible for Rap1- and RAPL-dependent integrin regulation (Katagiri et al., 2006, 2009). Mst1 is also involved in T cell proliferation (Avruch et al., 2009; Katagiri et al., 2009). Proliferative responses were augmented in *Mst1*$^{-/-}$ T cells, but not B cells (Avruch et al., 2009; Katagiri et al., 2009). However, p27 regulation in *Mst1*$^{-/-}$ lymphocytes was found to be normal (unpublished data). Thus, Mst1 differently regulates lymphocyte proliferation independently of p27, and hyperproliferative responses observed in *Cdkn1b*$^{S10A/S10A}$ RAPL-deficient T cells might be due to defective activation of Mst1 by RAPL deficiency.

This study shows that KIS appears to be a relevant target of RAPL during the G1-S transition, because KIS phosphorylates S10 during the G1 phase in response to mitogenic stimulation and promotes its nuclear export (Boehm et al., 2002). Interestingly, KIS was reported to play important roles in cell cycle

Figure 7. Effects of S10A Mutation on RAPL-Deficient Mice

(A) Expression of RAPL, p27, phospho-S10 of p27, and tubulin in B cells derived from *Cdkn1b*$^{+/+}$*Rassf5*$^{exon3+/exon3+}$, *Cdkn1b*$^{S10A/S10A}$*Rassf5*$^{exon3+/exon3+}$, and *Cdkn1b*$^{S10A/S10A}$*Rassf5*$^{exon3-/exon3-}$ mice.

(B) The ratios of CD138$^+$ and B220$^+$ lymphocytes (top left) or CD44$^+$ and CD62L$^-$ on CD4$^+$ gated lymphocytes (bottom left) from spleens of *Cdkn1b*$^{+/+}$*Rassf5*$^{exon3+/exon3+}$, *Cdkn1b*$^{+/+}$*Rassf5*$^{exon3-/exon3-}$, and *Cdkn1b*$^{S10A/S10A}$*Rassf5*$^{exon3-/exon3-}$ mice at 10 months of age. Flow cytometric profiles of expression of CD138 and B220 (top right) and CD44 and CD62L on CD4$^+$ gated lymphocytes (bottom right). *$p < 0.02$, **$p < 0.05$.

(C) Anti-double-strand DNA titers in 12-month-old *Cdkn1b*$^{+/+}$*Rassf5*$^{exon3+/exon3+}$, *Cdkn1b*$^{+/+}$*Rassf5*$^{exon3-/exon3-}$, and *Cdkn1b*$^{S10A/S10A}$*Rassf5*$^{exon3-/exon3-}$ (left). Proteinuria in 12-month-old mice (right). Proteinuria was measured with medical color strips. p values for *Cdkn1b*$^{S10A/S10}$*Rassf5*$^{exon3-/exon3-}$ mice compared to *Cdkn1b*$^{+/+}$*Rassf5*$^{exon3-/exon3-}$ mice are indicated on the graph. *$p < 0.02$, **$p < 0.01$.

(D) Development of B cell lymphomas in *Cdkn1b*$^{+/+}$*Rassf5*$^{exon3+/exon3+}$, *Cdkn1b*$^{+/+}$*Rassf5*$^{exon3-/exon3-}$, and *Cdkn1b*$^{S10A/S10A}$*Rassf5*$^{exon3-/exon3-}$ mice at 12 months of age. Lymph nodes and spleens from 20 mice per each group were subjected for histological examination.

(E) Left: The S10A mutation abrogated mislocalization of p27 with anti-IgM F(ab′)$_2$. Redistribution of p27 in B cells from *Cdkn1b*$^{+/+}$*Rassf5*$^{exon3+/exon3+}$, *Cdkn1b*$^{S10A/S10A}$*Rassf5*$^{exon3+/exon3+}$, and *Cdkn1b*$^{S10A/S10A}$*Rassf5*$^{exon3-/exon3-}$ mice. Primary B cells were stimulated with anti-IgM F(ab′)^2 for 2 hr and stained for p27 and nuclei (DAPI). Scale bars represent 5 μm. Right: The S10A mutation abrogated hyperproliferation of RAPL-deficient B cells with anti-IgM F(ab′)$_2$. ^{3}[H]-thymidine uptake by B cells. Primary B from *Cdkn1b*$^{+/+}$*Rassf5*$^{exon3+/exon3+}$, *Cdkn1b*$^{S10A/S10A}$*Rassf5*$^{exon3+exon3/+}$, *Cdkn1b*$^{S10A/S10A}$*Rassf5*$^{exon3-/exon3-}$, and *Cdkn1b*$^{+/+}$*Rassf5*$^{exon3-/exon3-}$ mice were unstimulated (–) or stimulated with anti-IgM F(ab′)$_2$ at concentrations indicated.

(F) Left: The S10A mutation corrected mislocalization of p27 with anti-CD3 and anti-CD28. Redistribution of p27 in T cells from *Cdkn1b*$^{+/+}$*Rassf5*$^{exon3+/exon3+}$, *Cdkn1b*$^{S10A/S10A}$*Rassf5*$^{exon3+/exon3+}$, and *Cdkn1b*$^{S10A/S10A}$*Rassf5*$^{exon3-/exon3-}$ mice. Primary T cells were stimulated with anti-CD3 and anti-CD28 for 2 hr and stained for p27 and nuclei (DAPI). Scale bars represent 5 μm. Right: The S10A mutation decreased hyperproliferative responses of RAPL-deficient T cells with anti-CD3 and anti-CD3+CD28. ^{3}[H]-thymidine uptake by T cells. Primary T from *Cdkn1b*$^{+/+}$*Rassf5*$^{exon3+/exon3+}$, *Cdkn1b*$^{S10A/S10A}$*Rassf5*$^{exon3+/exon3+}$, *Cdkn1b*$^{S10A/S10A}$*Rassf5*$^{exon3-/exon3-}$, and *Cdkn1b*$^{+/+}$*Rassf5*$^{exon3-/exon3-}$ mice were unstimulated (–) or stimulated with anti-CD3 and anti-CD3$^+$CD28. *$p < 0.01$, **$p < 0.03$.

progression of leukemia cell lines through the promotion of S10 phosphorylation of p27 (Nakamura et al., 2008), suggesting an important role of KIS in lymphoid cells. However, multiple kinases besides KIS were also reported to phosphorylate p27 at S10 including Cdk5 (Kawauchi et al., 2006), suggesting a complex network of redundant kinases controlling p27 degradation and cell cycle progression in vivo. It will be important to examine whether RAPL could regulate KIS and other kinase activities in lymphocytes.

The importance of RAPL regulation in the cell cycle is supported by the incidence of lupus-like glomerulonephritis disease. Although RAPL-deficient mice are lymphopenic at a young age, both RAPL-deficient T and B cells are activated and differentiate into effector-memory T cells and plasma cells with age. In a lymphopenic state, self-antigens provide proliferation-inducing signals that expand T cells until the T cell pool is reestablished to a nearly normal size (Lawson et al., 2001). It is conceivable that a lymphopenic state resulting from defective lymphocyte trafficking in RAPL-deficient mice favors homeostatic proliferation of self-reactive clones, which predisposes mice to autoimmune disease. IL-7 is critical for homeostatic proliferation together with signals from the TCR recognizing a complex of self-peptides and MHC (Jacobs et al., 2010; Tan et al., 2001). IL-7 might help expanding self-reactive clones in RAPL-deficient mice.

Enhanced lymphocyte proliferation probably increases the development of spontaneous B cell lymphomas in RAPL-deficient mice. RAPL-deficient mice also developed lung and liver tumors after 1.5 yr of age, suggesting a tumor-suppressor function for RAPL in nonlymphoid organs, despite low RAPL expression in these tissues. There are several studies showing that cytoplasmic p27 is associated with hyperproliferation and tumorigenesis through a cyclin-Cdk-independent function (Besson et al., 2006, 2007). Cytoplasmic mislocalization of p27 might underlie the development of spontaneous tumors in RAPL-deficient mice. It was also reported that the *NORE1B* (*RASSF5C*) gene was frequently inactivated in human hepatocellular carcinomas because of promoter methylation (Macheiner et al., 2006). It will be interesting to study involvement of downregulation of RAPL in human hyperproliferative autoimmune and malignant diseases.

Our findings that RAPL, a molecule originally identified as an integrin regulator, also plays an inhibitory role in cell proliferation provides a molecular link with cell adhesion and growth. In line with this notion, a constitutively active LFA-1 was found to be rather inhibitory to antigen-induced proliferation (Semmrich et al., 2005). Rap1 and p27 were previously reported to be involved in T cell anergy (Boussiotis et al., 2000). Recent studies suggest that cytoplasmic p27 can inhibit cell migration behaviors by binding to Rho or stathmin (Baldassarre et al., 2005). Further characterization of these processes will facilitate our understanding on the link between cell adhesion and proliferation thorough RAPL. Our studies provide important clues and experimental systems to elucidate how disruption of coordinated regulation of adhesion and proliferation leads to autoimmunity and carcinogenesis.

EXPERIMENTAL PROCEDURES

Plasmids, antibodies, and reagents are described in Supplemental Experimental Procedures.

Mice

RAPL-deficient mice were generated by targeting the RAPL-specific exon3 of *Rassf5* as previously described (Katagiri et al., 2004). Homozygous mice and littermate control mice were crossed with wild-type C57BL/6 mice for eight generations. Mice were housed in specific-pathogen-free conditions and all experiments were in accordance with protocols approved by the Animal Care and Use Committee of Kansai Medical University (Osaka, Japan). p27 genetically targeted mice harboring an S10A mutation were generated as previously described (Kotake et al., 2005).

Immunoprecipitation, Immunoblot, and In Vitro Kinase Assays

Immunoprecipitation and immunoblot were performed as described in Supplemental Experimental Procedures. Signals of appropriate bands were quantified with an image analyzer (BAS-1500, Fujifilm). Kinase assays for Cdk2 and Cdk4 were performed as described before (Nakayama et al., 1996). In brief, immunoprecipitates with rabbit anti-Cdk2 or anti-Cdk4 from cell lysates from T or B cells stimulated with anti-IgM $(Fab')_2$ or anti-CD3 and anti-CD28 were washed with lysis buffer (Nonidet P-40, 150 mM NaCl, 25 mM Tris-HCl [pH 7.4], 10% glycerol) and suspended in 30 μl of kinase buffer (50 mM HEPES [pH 7.4], 10 mM $MgCl_2$, 1 mM DTT, 10 mM β-glycerophosphate) containing 1 μg Histone H1 (Calbiochem) or 0.5 μg GST-Rb (Santa-Cruz) and 25 μM ATP, 10 μCi [γ-^{32}P]ATP (6000 Ci/mmol, Amersham). The samples were incubated at 30°C for 30 min, denatured in SDS sample buffer, and run on a 15% SDS-polyacrylamide gel (Nakayama et al., 1996). Kinase assays of KIS were done with GST-p27 and GST-p27S10A, as described (Boehm et al., 2002). The signals from appropriate bands were quantified with a phosphoimager (BAS3000, Fujifilm) and fold-increase was calculated after background subtraction.

Immunostaining

Immunostaining procedures are described in Supplemental Experimental Procedures. Confocal images were obtained with a LSM510 META microscope with a 63× objective lens. Line profiles of cells stained for p27 and nuclei (DAPI) were used to measure nuclear/cytoplasmic p27 distribution (see Supplemental Experimental Procedures and Figure S3 for details). Cell surface staining and analysis with a FACSCalibur (Beckton-Dickinson) flow cytometer were previously described (Katagiri et al., 2004). For immunohistochemistry of kidney tissues to detect IgG and C3 deposition, paraffin sections were dewaxed, blocked with diluted horse serum, and then stained with FITC-goat anti-mouse IgG and C3.

Cell Proliferation and BrdU Incorporation Assays

B and T lymphocytes purified from spleens or lymph nodes were cultured at 1.5 × 10^5/ml in 0.2 ml per well of a 96-well plate with or without anti-IgM $F(ab')_2$ or anti-CD3(5 μg/ml and CD28 (2 μg/ml) for 48 hr. [^{3}H]-thymidine (1 μmCi/well) was added for the last 6 hr. Cells were harvested and [^{3}H]-thymidine uptake was measured. To determine the frequency and nature of individual cells that synthesized DNA during culture, BrdU incorporation was performed with a BrdU flow kit according to the manufacturer's instruction (BD PharMingen). BrdU uptake in vivo is described in Supplemental Experimental Procedures.

Statistical Analysis

Student's two-tailed t test was used to compare experimental groups. p values less than 0.05 were considered significant.

SUPPLEMENTAL INFORMATION

Supplemental Information includes Supplemental Experimental Procedures and seven figures and can be found with this article online at doi:10.1016/j.immuni.2010.12.010.

ACKNOWLEDGMENTS

We would like to thank S. Matsuda (Kansai Medical University, Japan) for critical reading of the manuscript and S. Ohishi, K. Maebara, and R. Hamaguchi for technical assistance. This research was supported by grants-in-aid from the Ministry of Education, Culture, Sports, Science and Technology of

Japan and the Ministry of Health, Labor and Welfare, and from CREST Japan Science and Technology Agency, and research grants from Takeda Science Foundation, Yasuda Medical foundation, Japan Leukemia Research Fund, and Astellas Foundation for Research on Metabolic Disorders.

Received: May 11, 2010
Revised: September 25, 2010
Accepted: December 15, 2010
Published online: December 30, 2010

REFERENCES

Aleem, E., Kiyokawa, H., and Kaldis, P. (2005). Cdc2-cyclin E complexes regulate the G1/S phase transition. Nat. Cell Biol. *7*, 831–836.

Appleman, L.J., Berezovskaya, A., Grass, I., and Boussiotis, V.A. (2000). CD28 costimulation mediates T cell expansion via IL-2-independent and IL-2-dependent regulation of cell cycle progression. J. Immunol. *164*, 144–151.

Avruch, J., Xavier, R., Bardeesy, N., Zhang, X.F., Praskova, M., Zhou, D., and Xia, F. (2009). Rassf family of tumor suppressor polypeptides. J. Biol. Chem. *284*, 11001–11005.

Baldassarre, G., Belletti, B., Nicoloso, M.S., Schiappacassi, M., Vecchione, A., Spessotto, P., Morrione, A., Canzonieri, V., and Colombatti, A. (2005). p27 (Kip1)-stathmin interaction influences sarcoma cell migration and invasion. Cancer Cell *7*, 51–63.

Balomenos, D., and Martinez, A.C. (2000). Cell-cycle regulation in immunity, tolerance and autoimmunity. Immunol. Today *21*, 551–555.

Barnouin, K., Fredersdorf, S., Eddaoudi, A., Mittnacht, S., Pan, L.X., Du, M.Q., and Lu, X. (1999). Antiproliferative function of p27kip1 is frequently inhibited in highly malignant Burkitt's lymphoma cells. Oncogene *18*, 6388–6397.

Bashir, T., Dorrello, N.V., Amador, V., Guardavaccaro, D., and Pagano, M. (2004). Control of the SCF(Skp2-Cks1) ubiquitin ligase by the APC/C(Cdh1) ubiquitin ligase. Nature *428*, 190–193.

Besson, A., Gurian-West, M., Chen, X., Kelly-Spratt, K.S., Kemp, C.J., and Roberts, J.M. (2006). A pathway in quiescent cells that controls p27Kip1 stability, subcellular localization, and tumor suppression. Genes Dev. *20*, 47–64.

Besson, A., Hwang, H.C., Cicero, S., Donovan, S.L., Gurian-West, M., Johnson, D., Clurman, B.E., Dyer, M.A., and Roberts, J.M. (2007). Discovery of an oncogenic activity in p27Kip1 that causes stem cell expansion and a multiple tumor phenotype. Genes Dev. *21*, 1731–1746.

Bhattacharjee, R.N., Banks, G.C., Trotter, K.W., Lee, H.L., and Archer, T.K. (2001). Histone H1 phosphorylation by Cdk2 selectively modulates mouse mammary tumor virus transcription through chromatin remodeling. Mol. Cell. Biol. *21*, 5417–5425.

Boehm, M., Yoshimoto, T., Crook, M.F., Nallamshetty, S., True, A., Nabel, G.J., and Nabel, E.G. (2002). A growth factor-dependent nuclear kinase phosphorylates p27(Kip1) and regulates cell cycle progression. EMBO J. *21*, 3390–3401.

Bos, J.L., de Rooij, J., and Reedquist, K.A. (2001). Rap1 signaling: Adhering to new models. Nat. Rev. Mol. Cell Biol. *2*, 369–377.

Boussiotis, V.A., Freeman, G.J., Taylor, P.A., Berezovskaya, A., Grass, I., Blazar, B.R., and Nadler, L.M. (2000). p27kip1 functions as an anergy factor inhibiting interleukin 2 transcription and clonal expansion of alloreactive human and mouse helper T lymphocytes. Nat. Med. *6*, 290–297.

Ebisuno, Y., Katagiri, K., Katakai, T., Ueda, Y., Nemoto, T., Inada, H., Nabekura, J., Okada, T., Kannagi, R., Tanaka, T., et al. (2010). Rap1 controls lymphocyte adhesion cascade and interstitial migration within lymph nodes in RAPL-dependent and -independent manners. Blood *115*, 804–814.

Ekholm, S.V., and Reed, S.I. (2000). Regulation of G(1) cyclin-dependent kinases in the mammalian cell cycle. Curr. Opin. Cell Biol. *12*, 676–684.

Fero, M.L., Rivkin, M., Tasch, M., Porter, P., Carow, C.E., Firpo, E., Polyak, K., Tsai, L.H., Broudy, V., Perlmutter, R.M., et al. (1996). A syndrome of multiorgan hyperplasia with features of gigantism, tumorigenesis, and female sterility in p27(Kip1)-deficient mice. Cell *85*, 733–744.

Hara, T., Kamura, T., Nakayama, K., Oshikawa, K., and Hatakeyama, S. (2001). Degradation of p27(Kip1) at the G(0)-G(1) transition mediated by a Skp2-independent ubiquitination pathway. J. Biol. Chem. *276*, 48937–48943.

Ishida, N., Kitagawa, M., Hatakeyama, S., and Nakayama, K. (2000). Phosphorylation at serine 10, a major phosphorylation site of p27(Kip1), increases its protein stability. J. Biol. Chem. *275*, 25146–25154.

Ishida, N., Hara, T., Kamura, T., Yoshida, M., Nakayama, K., and Nakayama, K.I. (2002). Phosphorylation of p27Kip1 on serine 10 is required for its binding to CRM1 and nuclear export. J. Biol. Chem. *277*, 14355–14358.

Jacobs, S.R., Michalek, R.D., and Rathmell, J.C. (2010). IL-7 is essential for homeostatic control of T cell metabolism in vivo. J. Immunol. *184*, 3461–3469.

Katagiri, K., Maeda, A., Shimonaka, M., and Kinashi, T. (2003). RAPL, a Rap1-binding molecule that mediates Rap1-induced adhesion through spatial regulation of LFA-1. Nat. Immunol. *4*, 741–748.

Katagiri, K., Ohnishi, N., Kabashima, K., Iyoda, T., Takeda, N., Shinkai, Y., Inaba, K., and Kinashi, T. (2004). Crucial functions of the Rap1 effector molecule RAPL in lymphocyte and dendritic cell trafficking. Nat. Immunol. *5*, 1045–1051.

Katagiri, K., Imamura, M., and Kinashi, T. (2006). Spatiotemporal regulation of the kinase Mst1 by binding protein RAPL is critical for lymphocyte polarity and adhesion. Nat. Immunol. *7*, 919–928.

Katagiri, K., Katakai, T., Ebisuno, Y., Ueda, Y., Okada, T., and Kinashi, T. (2009). Mst1 controls lymphocyte trafficking and interstitial motility within lymph nodes. EMBO J. *28*, 1319–1331.

Kawauchi, T., Chihama, K., Nabeshima, Y., and Hoshino, M. (2006). Cdk5 phosphorylates and stabilizes p27kip1 contributing to actin organization and cortical neuronal migration. Nat. Cell Biol. *8*, 17–26.

Kotake, Y., Nakayama, K., Ishida, N., and Nakayama, K.I. (2005). Role of serine 10 phosphorylation in p27 stabilization revealed by analysis of p27 knock-in mice harboring a serine 10 mutation. J. Biol. Chem. *280*, 1095–1102.

Lawson, B.R., Koundouris, S.I., Barnhouse, M., Dummer, W., Baccala, R., Kono, D.H., and Theofilopoulos, A.N. (2001). The role of alpha beta+ T cells and homeostatic T cell proliferation in Y-chromosome-associated murine lupus. J. Immunol. *167*, 2354–2360.

Lee, J.G., and Kay, E.P. (2007). Two populations of p27 use differential kinetics to phosphorylate Ser-10 and Thr-187 via phosphatidylinositol 3-Kinase in response to fibroblast growth factor-2 stimulation. J. Biol. Chem. *282*, 6444–6454.

Li, L., Iwamoto, Y., Berezovskaya, A., and Boussiotis, V.A. (2006a). A pathway regulated by cell cycle inhibitor p27Kip1 and checkpoint inhibitor Smad3 is involved in the induction of T cell tolerance. Nat. Immunol. *7*, 1157–1165.

Li, W.Q., Jiang, Q., Aleem, E., Kaldis, P., Khaled, A.R., and Durum, S.K. (2006b). IL-7 promotes T cell proliferation through destabilization of p27Kip1. J. Exp. Med. *203*, 573–582.

Macheiner, D., Heller, G., Kappel, S., Bichler, C., Stattner, S., Ziegler, B., Kandioler, D., Wrba, F., Schulte-Hermann, R., Zochbauer-Muller, S., and Grasl-Kraupp, B. (2006). NORE1B, a candidate tumor suppressor, is epigenetically silenced in human hepatocellular carcinoma. J. Hepatol. *45*, 81–89.

Nakamura, S., Okinaka, K., Hirano, I., Ono, T., Sugimoto, Y., Shigeno, K., Fujisawa, S., Shinjo, K., and Ohnishi, K. (2008). KIS induces proliferation and the cell cycle progression through the phosphorylation of p27Kip1 in leukemia cells. Leuk. Res. *32*, 1358–1365.

Nakayama, K., Ishida, N., Shirane, M., Inomata, A., Inoue, T., Shishido, N., Horii, I., and Loh, D.Y. (1996). Mice lacking p27(Kip1) display increased body size, multiple organ hyperplasia, retinal dysplasia, and pituitary tumors. Cell *85*, 707–720.

Polyak, K., Lee, M.H., Erdjument-Bromage, H., Koff, A., Roberts, J.M., Tempst, P., and Massague, J. (1994). Cloning of p27Kip1, a cyclin-dependent kinase inhibitor and a potential mediator of extracellular antimitogenic signals. Cell *78*, 59–66.

Qi, C.F., Xiang, S., Shin, M.S., Hao, X., Lee, C.H., Zhou, J.X., Torrey, T.A., Hartley, J.W., Fredrickson, T.N., and Morse, H.C., 3rd. (2006). Expression of the cyclin-dependent kinase inhibitor p27 and its deregulation in mouse B cell lymphomas. Leuk. Res. *30*, 153–163.

Raab, M., Wang, H., Lu, Y., Smith, X., Wu, Z., Strebhardt, K., Ladbury, J.E., and Rudd, C.E. (2010). T cell receptor "inside-out" pathway via signaling module SKAP1-RapL regulates T cell motility and interactions in lymph nodes. Immunity *32*, 541–556.

Reynisdottir, I., and Massague, J. (1997). The subcellular locations of p15 (Ink4b) and p27(Kip1) coordinate their inhibitory interactions with cdk4 and cdk2. Genes Dev. *11*, 492–503.

Rodier, G., Montagnoli, A., Di Marcotullio, L., Coulombe, P., Draetta, G.F., Pagano, M., and Meloche, S. (2001). p27 cytoplasmic localization is regulated by phosphorylation on Ser10 and is not a prerequisite for its proteolysis. EMBO J. *20*, 6672–6682.

Semmrich, M., Smith, A., Feterowski, C., Beer, S., Engelhardt, B., Busch, D.H., Bartsch, B., Laschinger, M., Hogg, N., Pfeffer, K., and Holzmann, B. (2005). Importance of integrin LFA-1 deactivation for the generation of immune responses. J. Exp. Med. *201*, 1987–1998.

Sherr, C.J., and Roberts, J.M. (1999). Cdk inhibitors: Positive and negative regulators of G1-phase progression. Genes Dev. *13*, 1501–1512.

Stork, P.J., and Dillon, T.J. (2005). Multiple roles of Rap1 in hematopoietic cells: Complementary versus antagonistic functions. Blood *106*, 2952–2961.

Tan, J.T., Dudl, E., LeRoy, E., Murray, R., Sprent, J., Weinberg, K.I., and Surh, C.D. (2001). IL-7 is critical for homeostatic proliferation and survival of naive T cells. Proc. Natl. Acad. Sci. USA *98*, 8732–8737.

Vos, M.D., Martinez, A., Ellis, C.A., Vallecorsa, T., and Clark, G.J. (2003). The pro-apoptotic Ras effector Nore1 may serve as a Ras-regulated tumor suppressor in the lung. J. Biol. Chem. *278*, 21938–21943.